

Learning Effects in Coupled Arrays of Cellular Neural Oscillators

Robert Kozma · Marko Puljic

Received: 14 May 2012 / Accepted: 7 August 2012 / Published online: 23 August 2012
© Springer Science+Business Media, LLC 2012

Abstract We analyze spatio-temporal dynamics of coupled neural oscillatory arrays. The interconnected oscillators can produce a wide range of dynamics, including quasi-periodic limit cycles, chaotic waveforms, and intermittent chaotic oscillations. We study the role of distributed input bias and develop methods for learning the input patterns. After learning, the coupled oscillators produce large-scale synchronized, narrow-band oscillations in response to the learned patterns. We study patterns of amplitude modulations that span the whole lattice graph. The presented results correspond to Freeman's 6th building block of neurodynamics.

Keywords Cellular neural networks · Coupled oscillators · Chaos · Hebbian learning · Freeman K-sets · Phase transition

Introduction

In mammalian olfaction, inhalations bring odorants to the nose and excite a small subsets of the specialized receptor neurons. Among thousand types of receptors, a small fraction of each kind is excited on each inhalation, so a sparse spatial pattern of pulses is sent to the olfactory bulb with each intake of air [5]. Other background odorants

come too, so the sparse pattern is buried into noisy input and bulb needs to detect a desired stimulus. The spatial pattern of receptor pulses differs for each inhalation, even for the same odorant. This variability is observed in the other sensory systems as well, but despite this variability, the recognition works fine. Patterns projected on bulbar neurons are as variable as the receptor patterns, because there is only a single synapse between the receptor axons and the bulbar neurons. But a spatial pattern of bulbar activity is almost invariant over many intakes of the same odorant. This pattern covers the entire bulb, and every neuron in the bulb is involved with every pattern presentation. The pattern in the bulb is carried through the high-frequency γ range oscillations [6].

In this work, we want to model six important building blocks of olfactory system capable of pattern recognition. Our graph model has vertices that have two states 0 and 1 and follow their neighbors' states more likely, and edges that inhibit or excite [11, 12]. Graph has to show following six building blocks of neuron-inspired dynamics [1, 4]:

First, when each neuron projects the most common influences it receives, the neurons cease to act individually and their activity level is determined by the population. This transition is the first building block of neuron-inspired dynamics.

Second, when two populations of neurons are coupled with inhibitory connection and when they are temporarily excited, then the populations' activity oscillates, but returns to the basal levels without additional excitation. This form of oscillation is the second building block of neuron-inspired dynamics.

Third, when synaptic strength among neurons increases enough, temporarily excited populations of neurons return to the basal oscillatory behavior. Self-sustained oscillation is the third building block of neuron-inspired dynamics.

R. Kozma (✉)
University of Memphis, Memphis, TN, USA
e-mail: rkozma@memphis.edu

M. Puljic
Tulane University, New Orleans, LA, USA
e-mail: mpuljic@tulane.edu

Fourth, the olfactory bulb made of coupled oscillatory populations of neurons shows continual self-stabilizing background activity with aperiodic waveforms, which is the fourth building block of neuron-inspired dynamics.

Fifth, with the inhalation or input, there is a burst of activity. The burst is all over the bulb and the same instantaneous frequency. The oscillations are due to the negative feedback interactions, and the shared frequency is due to the widespread interconnections between the neurons by which every neuron reaches every other in a few synapses. The common wave has a different amplitude at each location in the bulb and the wave serves as a carrier wave in the γ range, with a spatial pattern of amplitude modulation (AM) throughout the bulb. This is a carrier wave because the waveform is the same everywhere but its amplitude varies. The AM pattern is the fifth building block of neuron-inspired dynamics. Contour plots of amplitudes of activity in the bulb give a simple way of representing the state of the bulb. They are never quite the same, but we can easily discriminate from the patterns of other states.

Sixth, input from the receptors forms bulbar bursts, which increases bulbar wave activity. The input also increases the gain or the strength of the synaptic actions of the neurons. The higher the gain, the more prolonged are the oscillations. The state transitions into and out of a burst start and finish the first full step of perception into the bulb. This destabilization by input-dependent gain is the sixth building block of neuron-inspired dynamics.

Model and its Evolution

A vertex $v_i \in V$ of a graph $G(V, E)$ is in one of the two states, $s(v_i)$, inactive and active (0 and 1), and with $d(v_i)$ neighbors influencing it through the edges. Edge from v_i to v_j , $v_i v_j \in E$, can excite and inhibit. Excitatory edges project the states of neighbors, and inhibitory edges project the opposite states of neighbors, 0 if the neighbor's state is 1, and 1 if it is 0. Vertex's state, influenced by edges, is determined by the majority rule; when the most neighbors are active, the higher a chance for the vertex to be active, and when the most neighbors are inactive, the higher a chance for the vertex to be inactive (Fig. 1 down).

Evolution and Activation

At time $t = 0$ $s(v_i)$ is randomly set to 0 or 1. Then, for $t = 1, 2, \dots, T - 1$, a majority rule is applied simultaneously over all vertices. A vertex v_i is influenced by a state of its each neighbor $v_j \in N(v_i)$, whenever a random variable $R(v_i, t)$ is less than edge strength, $\omega_{j,i}$, of the

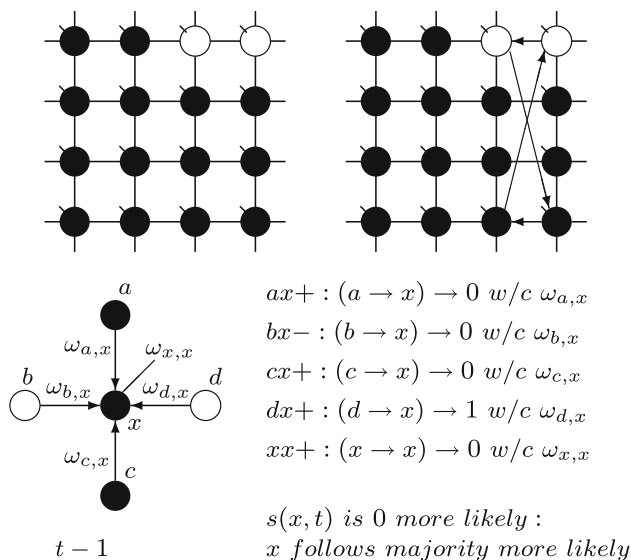


Fig. 1 Up-left: 2D torus of order 4×4 . In the 2D torus, the first row/column is connected with last row/column. Each vertex has a self-influence. Up-right: 2D torus after the basic random rewiring strategy. Two out of eighty (16×5) edges are rewired or 2.5 %. Down: An example of how majority function works. bx edge inhibits with strength $\omega_{b,x}$, so it sends 0 when $s(b, t - 1) = 1$. Given the scenario, $s(x, t)$ is 0 most likely

influencing excitatory edge $v_j v_i$, else the vertex v_i is influenced by an opposite state of neighbor v_j . If the edge $v_j v_i$ is inhibitory, the vertex v_j sends 0 when $s(v_j) = 1$, and 1 when $s(v_j) = 0$. Then, a vertex v_i gets a state of the most common influence, if there is such, otherwise a vertex state is randomly set to 0 or 1. Formula for the majority rule:

$$s(v_i, t) = \begin{cases} 0 & \text{if } \sum_{v_j \in N(v_i)} f(v_j, t) < \frac{d(v_i)}{2} \\ 1 & \text{if } \sum_{v_j \in N(v_i)} f(v_j, t) > \frac{d(v_i)}{2} \\ 0 \text{ or } 1 & \text{if } \sum_{v_j \in N(v_i)} f(v_j, t) = \frac{d(v_i)}{2} \end{cases} \quad (1)$$

$$f(v_j, t) = \begin{cases} 0 & \text{if } \omega_{j,i}(s(v_j, t - 1) = 0) \geq R(v_i, t); \text{ else } 1 \\ 1 & \text{if } \omega_{j,i}(s(v_j, t - 1) = 1) \geq R(v_i, t); \text{ else } 0 \end{cases}$$

$$s(v_j, t - 1) = \begin{cases} 0 & \text{if } \omega_{j,i}(s(v_j, t - 1) = 0) \text{excites}; \text{ else } 1 \\ 1 & \text{if } \omega_{j,i}(s(v_j, t - 1) = 1) \text{excites}; \text{ else } 0 \end{cases}$$

$$0 \leq R(v_i, t) \leq 1$$

$$0.5 \leq \omega_{j,i}(s(v_j)) \leq 1$$

The most basic parameter describing the finite graph G dynamics is its activation, $S_a(G, t)$, and its activation per vertex, $a(G, \omega)$, at time t :

$$S_a(G, t) = \sum_{i=0}^{|V|-1} s(v_i) \tag{2}$$

$$a(G, t) = \frac{S_a(G, t)}{|V|} \tag{3}$$

$$\langle a \rangle = \frac{\sum_{t=0}^{T-1} a(G, t)}{T} \tag{4}$$

Graph Structure to Model Olfaction

Graph Over Two-dimensional Lattice

Lattice-like graphs are built by randomly re-connecting some edges in the graphs set on a regular grid in D dimensions and folded into tori. In the basic random rewiring strategy, n directed edges from $n \times 2$ vertices are plugged out from a graph randomly. At that point, the graph has n vertices lacking an incoming edge and n vertices lacking an outgoing edge. To preserve the vertex degrees of the original graph, the set of plugged-out edges is returned back to the vertices with the missing edges in the random order. An edge is pointed to the vertex missing the incoming edge and is projected from the vertex missing the outgoing edge (Fig. 1 up).

Oscillators of Two Coupled Lattices

Oscillator is a graph made out of two connected lattice-like subgraphs (Fig. 2). Inhibitory subgraph G_1 projects toward the other excitatory subgraph G_0 the edges that inhibit, and G_0 projects toward G_1 the edges that excite. An edge from G_1 influences the vertex of G_0 with 1 when inactive and with 0 when active. An edge from G_0 influences the vertex of G_1 with 1 when active and with 0 when inactive.

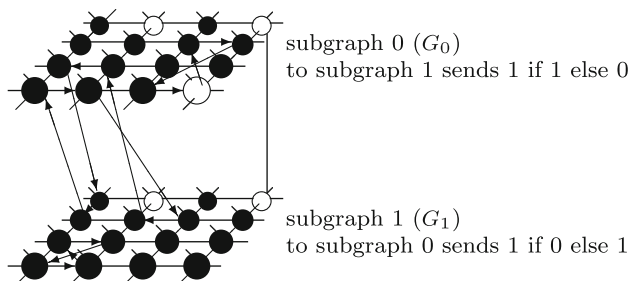


Fig. 2 Example of an oscillator. Two coupled subgraphs and each with four out of eighty (5 %) edges rewired. In each of two subgraphs, G_0 and G_1 , two edges are rewired within the subgraph and two edges are rewired to the other subgraph to couple. Within a subgraph, the edges are excitatory. Edges from G_0 to G_1 are excitatory and edges from G_1 to G_0 are inhibitory

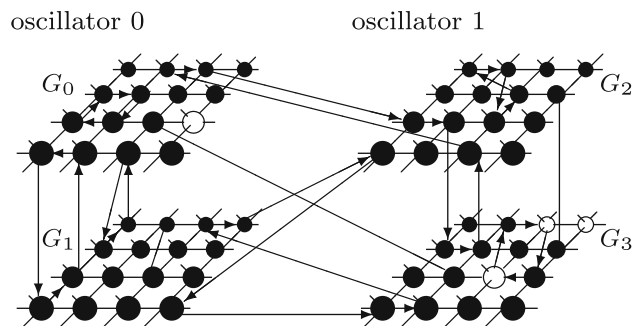


Fig. 3 Example of two coupled oscillators with four subgraphs G_0 , G_1 , G_2 , and G_3 . Each subgraph has six edges rewired or 7.5 %. Each subgraph has two edges rewired within itself. G_0 has two edges rewired with G_1 to couple into an oscillator. G_2 and G_3 are also coupled with two rewired edges. One edge from a subgraph is rewired to the each of the remaining subgraphs. Edges from G_1 and G_3 to G_0 or G_2 are inhibitory. Other edges are excitatory

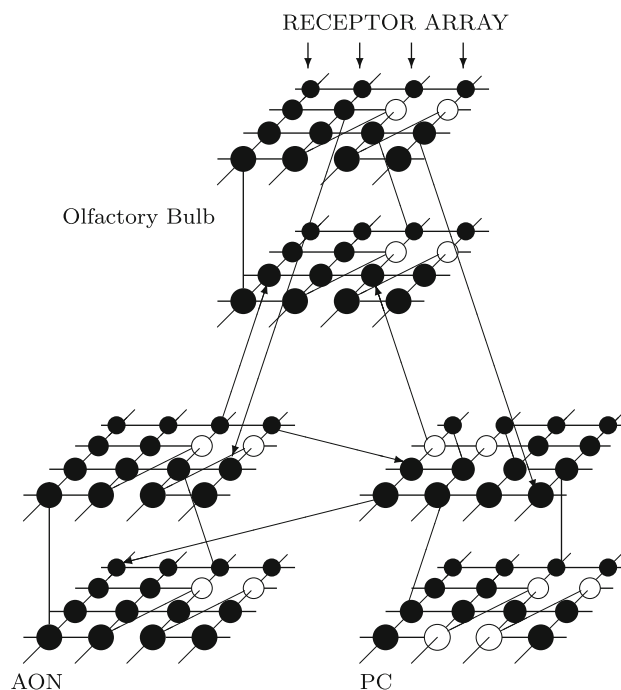


Fig. 4 An example of schematic view of the multi-layer structure of K3 representing olfactory system. There are excitatory–inhibitory pairs of layers in the olfactory bulb (mitral and granule layers), the anterior olfactory nucleus (AON), and the prepyriform cortex (PC)

Two Coupled Oscillators

In two oscillators, there are four subgraphs interconnected to form graph $G = G_0 \cup G_1 \cup G_2 \cup G_3$. Subgraph G_0 and G_1 are coupled into one oscillator and G_2 and G_3 into the other. There are additional edges between G_0 and G_1 that connect to both G_2 and G_3 . Edges from G_1 and G_3 are inhibitory if they project to G_0 or G_2 . All the other edges are excitatory (Fig. 3).

Example of 3 Coupled Oscillators

There are many possible oscillator couplings, but one useful inspiration comes from Freeman's K-sets, which model chaotic behavior and are inspired by biological system [4]. K-sets are derived primarily from observations of the olfactory system (Fig. 4), and they can be represented by coupled dynamic subgraphs.

Dynamics of Lattice-like Graph and an Oscillator

Critical Behavior of 2D Lattice Graphs

Depending on the strength of ω , a lattice-like graph is in the one of two possible regimes (Fig. 5 top) [3, 12, 13]. In the first regime, vertex states 0 and 1 are equiprobable, and graph's a distribution is uni-modal. In the second regime, one state dominates; vertex states are mostly 0 or mostly 1, and graph's a distribution is bi-modal. These two regimes are separated by a transition point, where a graph is very unstable. After the transition point, vertices cease to act individually and become a part of a group. Their activity level is determined by the population. The threshold for this state or regime transition is reached when each vertex,

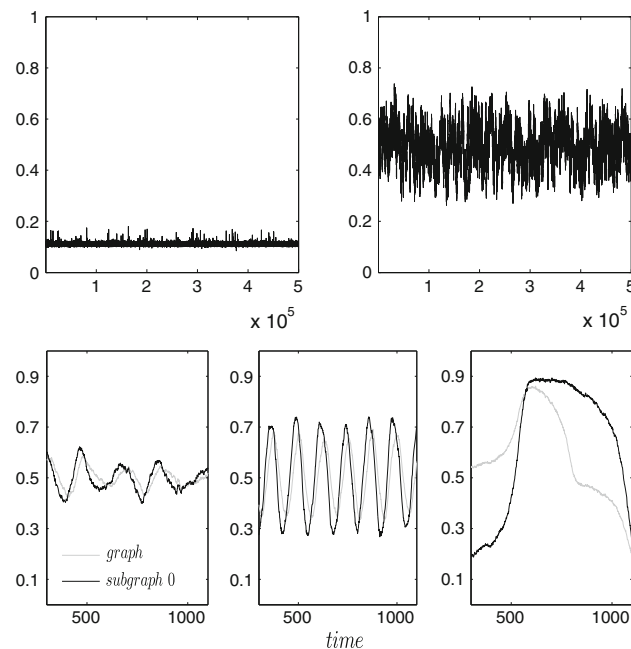


Fig. 5 Example of dynamics of 2D torus and oscillator made of two lattice-like subgraphs. Top: There are 2 distinct graph's regimes; one without dominant activation, and the other with dominant activation. Down: Demonstration of three different modes in oscillator $G(5, 3.75\%)$ made of two 2D torus rewired subgraphs G_0 and G_1 of order 96×96 . Each subgraph has 2304 (5%) edges rewired within and 1728 (3.75%) edges rewired toward the other subgraph

most likely, projects the most common influences it receives and this transition is the first building block of neuron-inspired dynamics.

Narrow-Band Oscillations in Coupled Lattices

Inhibitory connections in coupled subgraphs can generate oscillations and multi-modal activation states. Oscillator can be in three possible regimes, depending on ω (Fig. 5 down) [14, 15]. After the first transition point, graph activation oscillations start. After the second transition point, the oscillations stop.

Input Bias and Learning Effects in Oscillators

Even for lower ω , vertices in an oscillator have potential to oscillate if they are excited. $a(G, \omega)$ values of temporarily excited graph oscillate, but return to the basal levels without additional excitation (Fig. 6). This form of oscillation is the second building block of neuron-inspired dynamics. When ω values increase enough, $a(G, \omega)$ of graph oscillates without additional perturbation; when oscillating graph is temporarily excited, it returns to the basal oscillatory behavior. Self-sustained oscillation is the third building block of neuron-inspired dynamics.

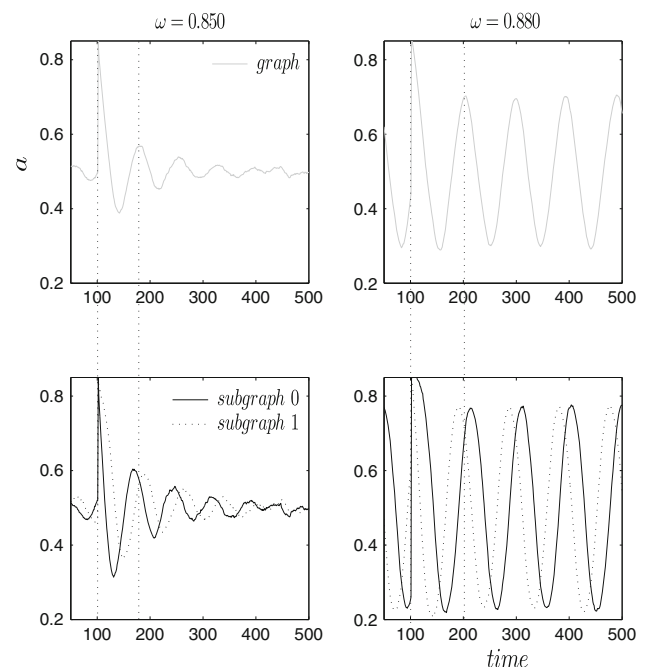


Fig. 6 Example of the second and third building block of neuron-inspired dynamics. Orders of 2D subgraphs are 200×200 , and in each subgraph, there are 10000 edges rewired and they are coupled with 20000 edges. Left: Excited graph starts to oscillate, but the oscillation decays and returns to the basal, non-oscillatory behavior. Right: Graph basal $a(G, \omega)$ is oscillatory

Three Coupled Oscillators

Three Oscillators in Isolation

Oscillators in isolation generate narrow-band limit cycle oscillation. Graphs with appropriate topology can model any frequency range. For example, an oscillator $O_0(5, 5\%) = G_0 \cup G_1$ made of 2D torus rewired subgraphs G_0 and G_1 having 5% edges rewired within and 5% edges rewired to couple each other, has different frequency form graphs $O_1(5, 7.5\%)$, and $O_2(5, 10\%)$ (Fig. 7).

Three Oscillators Interconnected

Every parameter describing a graph influences its behavior, and under appropriate conditions, interconnected oscillators with different frequencies cannot agree on a common mode, but together they can generate large-scale synchronization or chaotic background activity [8–10]. To observe the oscillator coupling effect, we interconnect three different oscillators $O_0(5, 5\%) = G_0 \cup G_1$, $O_1(5, 7.5\%) = G_2 \cup G_3$, and $O_2(5, 10\%) = G_4 \cup G_5$ by rewiring 1.25% edges from each of the subgraphs G_i to the remaining subgraphs G_j , $j \neq i$. Edges rewired from G_i to G_j with i odd and j even are inhibitory. All other edges are excitatory (Fig. 7). The oscillations of newly designed graph have a new form different from the oscillations.

Amplitude Modulation of Learned Pattern

We append input modeled by receptor vertices to three interconnected oscillators described previously, so our model resembles the one described in Fig. 4. Input from

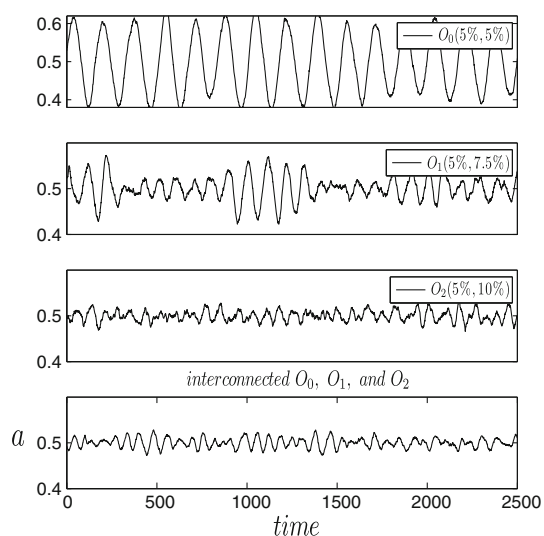


Fig. 7 Activation of three isolated oscillators and activation of three coupled oscillators (down)

receptor excites small subset of specialized vertices sensitive to the receptor type. Input is modeled by several hundred types of specialized vertices. When input to be learnt comes to pair of vertices simultaneously, so they are active at the same time, then the edges linking those vertices get stronger by increasing their ω values. This is a Hebb rule in which connections among the vertices that share activity get stronger [2, 7]. To recognize the learnt input, a smaller fraction of each kind of receptor is excited for each instance of input, so a sparse spatial pattern is sent to the coupled oscillators. Input representing the same object is always different at different times and many background excitations enter too, so the sparse input pattern is buried into noise. The job of coupled oscillators is to detect a desired pattern. And it does by increased oscillation (Fig. 8). The common wave of oscillation has a different amplitude at each location in the graph. The wave serves as a carrier wave and it has a spatial pattern of amplitude modulation (AM). The AM pattern is the fifth building block of neuron-inspired dynamics. Contour plots of AM provide a simple way of representing the state of the graph.

First Step of Perception

Input from the receptors forms bursts of activity in a graph, which increases the wave activity. The input also increases the strength of edges, thus enabling the more prolonged oscillations. The state transitions into and out of a burst is the first step of perception in the graph, and this destabilization is the sixth building block of neuron-inspired dynamics.

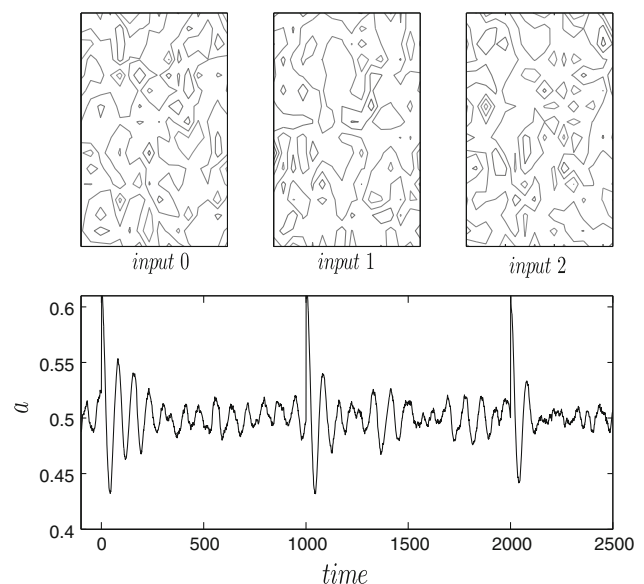


Fig. 8 Example of three different inputs and their AM patterns. Input increases the activity in a graph, which increases the oscillation

Conclusion

In a well-connected graph, vertices cease to act individually and their activity is determined by the group, which represents the first building block of neuron-inspired dynamics. With inhibitory connection, graph's activity oscillates after excitation, but returns to the basal levels. With the increase of edge strengths, oscillations are prolonged. These forms of oscillation are the second and third building block of neuron-inspired dynamics. Interconnected oscillators produce aperiodic or chaotic waveforms, which is the fourth building block of neuron-inspired dynamics. Patterns projected on coupled oscillators are variable, because there is only a single connection between the receptor vertices and the vertices in the three coupled oscillators, but the patterns of AM cover all the vertices in the graph, and every vertex is involved with AM pattern presentation. These AM contours represent a state of a graph, and they are fifth building block of neuron-inspired dynamics. The background activation is interrupted by burst of input, which drives graph to prolonged oscillation. This input-driven destabilization of chaotic background is the sixth building block on neuron-inspired dynamics.

Acknowledgments This work is supported in part by Defense Advanced Research Projects Agency (DARPA) Physical Intelligence Program in an HRL subcontract and by Air Force Office of Scientific Research (AFOSR) in the Mathematics and Cognition Program.

References

1. Aertsen A, Erb M, Palm G. Dynamics of functional coupling in the cerebral cortex: an attempt at a model-based interpretation. *Physica D Nonlinear Phenomena* 1994;75(1–3):103–128.
2. Aradi I, Barna G, Erdi P. Chaos and learning in the olfactory bulb. *Int J Intell Syst.* 1995;10:89.
3. Binder K. Finite size scaling analysis of Ising model block distribution functions. *Zeitschrift fur Physik B Condens Matter* 1981;43(2):119–140.
4. Freeman WJ. *Mass action in the nervous system.* New York: Academic Press; 1975.
5. Freeman WJ. Simulation of chaotic EEG patterns with a dynamic model of the olfactory system. *Biol Cybern* 1987;56(2–3):139–150.
6. Freeman WJ. *How brains make up their minds.* London: Weidenfeld and Nicolson; 1999.
7. Hebb DO. *The organization of behaviour.* New York: Wiley; 1949.
8. Kaneko K, Tsuda I. *Complex systems: chaos and beyond. A constructive approach with applications in life sciences.* Berlin: Springer; 2001.
9. Korn H, Faure P. Is there chaos in the brain? ii. Experimental evidence and related models. *CR Biol* 2003;326(9):787–840.
10. Kozma R, Freeman WJ. Chaotic resonance—methods and applications for robust classification of noisy and variable patterns. *Int J Bifurc Chaos* 2001;11(6):1607–1629.
11. Kozma R, Puljic M, Balister P, Bollobás B, Freeman WJ. Neuropercolation: A random cellular automata approach to spatio-temporal neurodynamics. *Lect Notes Comput Sci* 2004;3305:435–443.
12. Kozma R, Puljic M, Bollobás B, Balister PN, Freeman WJ. Phase transitions in the neuropercolation model of neural populations with mixed local and non-local interactions. *Biol Cybern* 2005;92(6):367–379.
13. Makowiec D. Stationary states of toom cellular automata in simulations. *Phys Rev E* 1999;60(4):3787–3796.
14. Puljic M, Kozma R. Narrow-band oscillations in probabilistic cellular automata. *Phys Rev E* 2008;78(026214):6.
15. Puljic M, Kozma R. Broad-band oscillations by probabilistic cellular automata. *J Cell Automata* 2010;5(6):491–507.